Climatology of Tropospheric Solitary Waves Observed over an Ice Shelf

Philip S. Anderson

British Antarctic Survey
Cambridge, UK
psan@bas.ac.uk

Abstract

Solitary-like wave events have been observed travelling through the lower troposphere over an Antarctic ice shelf. A catalogue of 73 events captured at Halley Station during the austral winter of 2003 implies that the waves are the remnants of micro-fronts or bores in the surface layer. The climatology of the direction of these events indicates that the wave generation mechanism is linked to flow over the surface and is not due to local orography. If this link is confirmed it suggests that the stable boundary layer has a self-induced horizontal complexity not previously recognised.

This paper is an introduction to a more substantial paper on ice shelf boundary-layer waves presently in preparation.

Keywords: Soliton, internal gravity waves, solitary wave, sodar, microbarograph, sonic anemometer, stable boundary layer, ice shelf.

1. Introduction

Internal Gravity Waves (IGWs) are ubiquitous features of stratified environmental fluids, being observed in oceans, lakes, the stratosphere and the stable atmospheric boundary layer (SBL). Gravity or buoyancy provides a restoring force within the fluid to any vertical displacement, whilst the density of the fluid provides the momentum term. Internal waves share some features of the more familiar surface (or interface) waves; both either grow as an instability within a shear-flow (e.g. wind ripples on the surface of lakes or oceans) or from an impulse (e.g. ripples spreading from a stone dropped into a pond).

Unlike interface wave, internal waves are frequently invisible, although cloud formations or fog can indicate their presence. Stratus clouds frequently exhibit wave-like structure, the vertical perturbation of the wave affecting the temperature and thence relative humidity to produce a stripped pattern in the sky. More dramatic are wave events that generate rather than merely modify clouds; mountain- or lee-waves give rise to lenticular clouds (Scorer 1949) whilst rotor-waves are the cause of the Morning Glory of Australia (Christie 1992).

Internal waves in the lower troposphere or boundary layer are less apparent than their stratospheric counterparts, for a variety of reasons. In the mid-latitudes (where most observations are made), the stratification required to maintain internal is relatively rare during daylight hours: indeed the SBL is frequently cited as the "nocturnal" boundary layer. A visualising tracer (e.g. cloud) is required, and although fog is not infrequent in the SBL, the typical horizontal scales pose a problem; a wave with a

typical length scale c. 100 m is not easy to observe from within a fog. Either the fog is too tenuous to observed wave structure, or too thick to see anything. Boundary-layer wave activity in fog is best seen from above: from a hill, high mast or aircraft, but such opportunities are relatively rare for the average observer. I am therefore indebted to Günther Heinemann for sending me the (I believe) unique photograph in figure 1, showing SBL waves over the Brunt Ice Shelf. The picture was taken through a Dornier aircraft window in December of 1990.

Figure 1. Photograph of a train of solitary-like waves over Brunt Ice Shelf made visible by shallow fog. The photograph was taken on 12th December, 1990, looking south out of the window of a Dornier aircraft flying just to the north of the ice cliffs (light band). The cliffs are ~30 m high. Image colour has been modified to enhance the contrast.

Numerical models of the atmosphere or ocean require an understanding of large scale internal waves in order to ensure correct partitioning of momentum transfer within the model scheme. Waves induced at the surface by large scale topography can transfer momentum vertically which manifests as an enhancement to drag. Internal waves have been studied intensively since the first computer models were developed in order to include internal wave drag correctly. Failure to do so results in highly unrealistic global and synoptic scale forecasts.

Studies of IGWs within the SBL are rare however. In part this is because the wave signature is often small compared to the back-ground turbulence, making measurements of the signal problematic. It is also because under the more common neutral or near neutral stratification, IGW activity appears to have minimal effect. Boundary layer models (which invariably exclude any IGW parameterisation) are only grossly "wrong" under moderate to extreme stability, and there is as yet no consensus to explain their poor performance: waves are one of a number of possibilities.

Are waves the hidden physics within the stratified boundary layer? In order to address this issue, the British Antarctic Survey deployed a set of micrometeorological instruments on the Brunt Ice Shelf as part of their studies of surface processes affecting climate. Part of the instrumentation set was aimed at measuring internal wave climatology and wave-turbulence interaction in the SBL.

The experiment ran during the austral winter of 2003 and was based at the Survey's Halley station (76°S 26°W), situated in the south Weddell Sea (figure 2). The site is ideal for stable boundary layer research, being flat, smooth and with an uninterrupted fetch of many kilometres in the predominant wind direction (King and Anderson 1988; King et al. 1989).

Wave climatology and wave-turbulence interaction studies had been carried out in previous campaigns at the same site using a variety of instruments, such as acoustic radar (King et al. 1987), arrays of wind vanes (Rees and Rottman 1994) and sonic anemometers (Rees et al. 1998). Field studies elsewhere show that internal waves are most readily detected by microbarographs (Anderson et al. 1992) and the instrumentation deployed for 2003 included an array of four microbarographs deployed as shown in figure 3. In addition to the microbarograph array, a monostatic acoustic radar (sodar) and 32-m turbulence mast provided near-surface measurements of the waves.

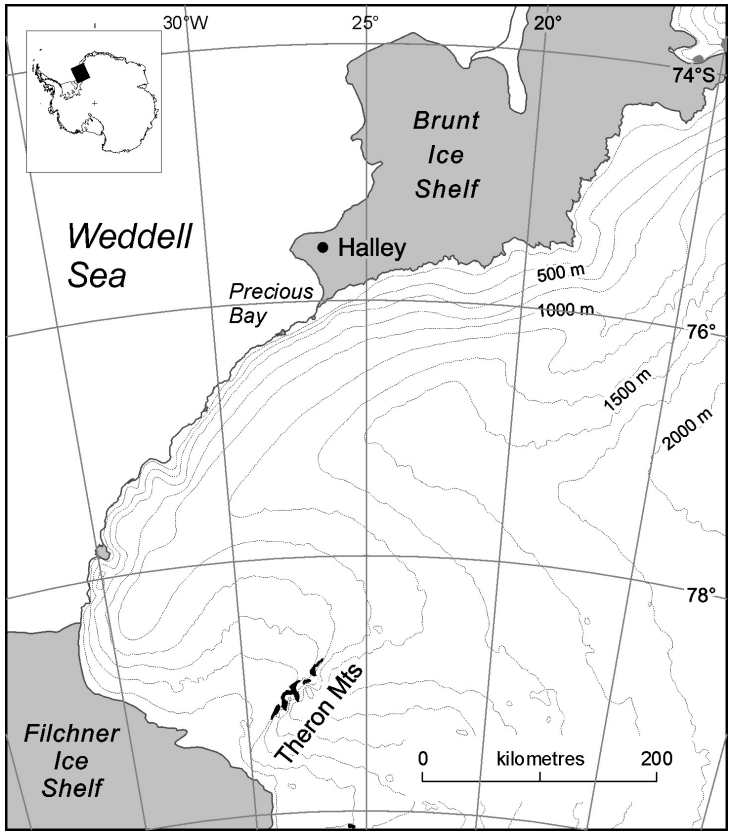

Figure 2. Map of the Brunt Ice Shelf and local topography around Halley. To the south-east of the station the continent rises to 2000 m with a mean slope of 1/100.

2. Methods

2.1. Microbarographs

Four microbarographs were deployed in an array as shown in Figure 3, the length scale of the array being ~300 m. The pressure sensors were buried in the porous snow, a technique which reduces turbulent pressure noise but does not degrade the wave signature (Anderson et al. 1992). Each sensor was able to resolve pressure changes of one millionth of an atmosphere (0.1 Pa).

The velocity of the wave signal relative to the surface (the extrinsic velocity) was calculated using trigonometry on the microbarograph positions along with the measured signature delay observed between each sensor. This assumes a parallel wave front, with the direction of the wave being defined as orthogonal to the assumed wave crest. The wave-signatures from each of the four array elements were invariably identical within the errors of noise, indicating minimal evolution of the signature as it crossed the array. The upper panel of figure 4 shows an example of the time series from the four microbarographs for a typical event. The four pressure measurements over-constrain the extrinsic velocity estimate and hence the range of values indicated confidence in the mean vector.

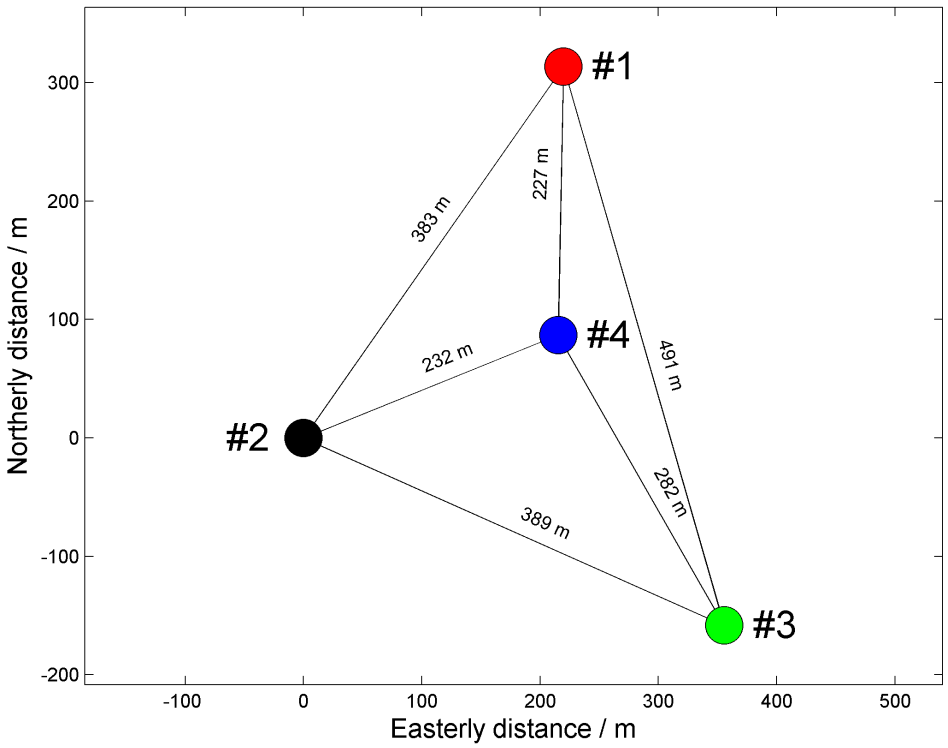

Figure 3. Layout of the microbarograph array. The sodar was co-located with sensor #2, and the turbulence mast was 1043 m south-east of #2 on a bearing of 147° True.

2.2. Sodar Echogrammes

A monostatic acoustic radar (sodar) was co-located with microbarograph #2 (figure 3). The sodar was a single axis unit recording profiles of acoustic backscatter (echogrammes) with a vertical resolution of two metre, capturing 500 m profiles every 10 s.

Sodar echogrammes are qualitative images of the intensity of turbulence coupled to the vertical temperature gradient. The Halley sodar was designed specifically to have a high vertical resolution in order to resolve fine scale turbulence structure (Anderson 2003); this structure manifests as layers of strong echo within weaker or undetectable echo. If conditions generate laminated echogrammes, the sodar data may also detect internal wave activity by the apparent short term vertical displacement of otherwise long lived structures. The central panel of figure 4 shows how the sodar signature is modified as the event passes over the site and how it correlates with the pressure signature of microbarograph #2.

Using sodar to visualise IGWs assumes that the backscatter texture is unaffected by the wave, that is, the existing backscatter acts as a passive tracer that is carried with the vertical movement of the air and is otherwise unmodified. Although plausible, there is some element of uncertainty in this assumption.

2.3. Micro-meteorological Data

A 32-m turbulence tower was situated 1043 m to the south-east of microbarograph #2 on a bearing of 147 degrees. The tower carried fast response sonic anemometers at nominal heights of 4m, 16m and 32m as well as other instrumentation not relevant to this paper. The sonic anemometers recorded three components of the wind vector [u,v,w] and temperature (T) at a sampling frequency of 20 Hz. Mean winds and fine scale structure were derived from the tower data, the former used in the calculation of the *intrinsic* velocity of the event, whilst the fine scale measurements indicated the near-surface flow structure of the wave.

The lower panel of figure 4 shows the wind vectors [u_{32}, v_{32}] from the uppermost anemometer for this event; these are the wind vectors after rotation to reduce mean v_{32} prior to the event to zero. Note that u_{32} is initially negative, but reduces to near calm within the event. Further, the shape of u_{32} is not identical to either the pressure or sodar signature in the panels above. These characteristics are repeated in most of the events indicating the excursion of the wind field from linearity.

Figure 5 shows two examples of the perturbation seen in the three wind components by two dissimilar waves; a typical deep wave on the left where the event affects all levels to a similar extent, and a rarer shallow wave on the right, where there is only a minimal residual effect at the 32 m level. In each case, however, the effect on the vertical wind, w, is similar, which is an integral from the surface of the diffluence of the horizontal wind, and manifests as the first derivative of the wind speed.

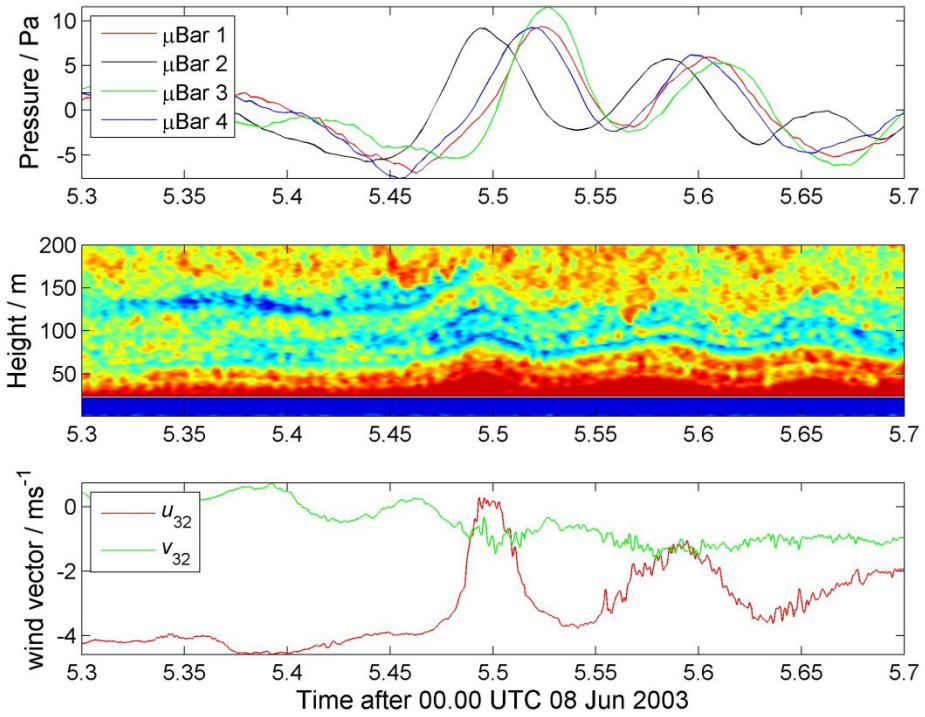

Figure 4. Examples of the effect of a train of solitary-like waves traversing the instrument array. The upper panel shows the four microbarograph time series; by referring to figure 3 it is clear this event came from ~WSW. The middle panel shows the effect of the event on the sodar echogramme, whilst the lower panel shows the horizontal components of the wind, rotated to give mean v = 0.

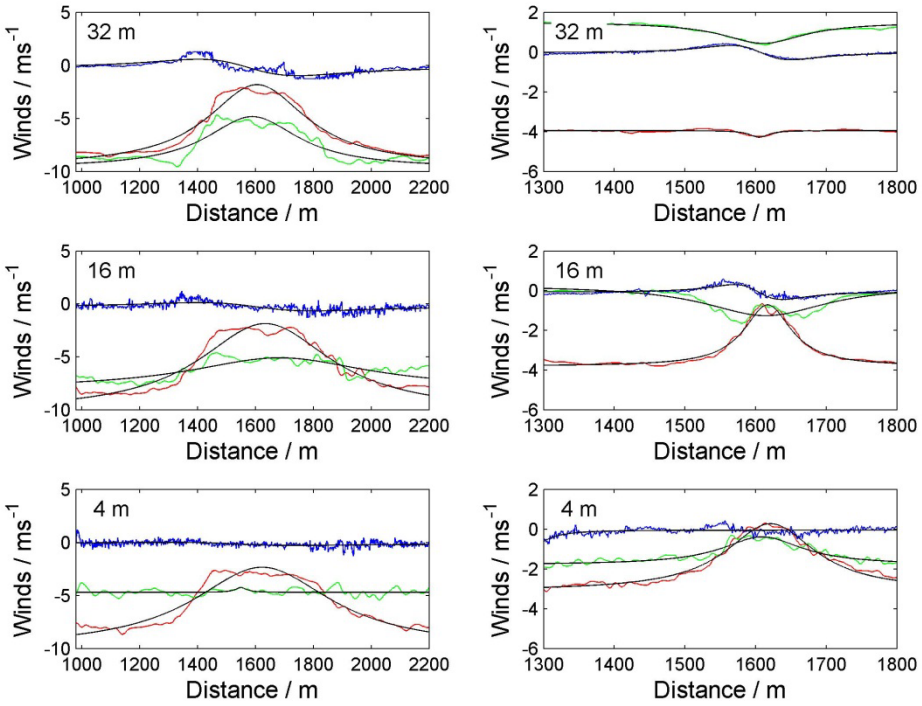

Figure 5. Two dissimilar events as observed at 4, 16 and 32 metre by sonic anemometers. The left-hand panels are for a deep wave, where [u, v] are affected relatively equally at all heights, and the vertical wind, w, shows the result of integrating the wind diffluence from the surface, that is, the w-perturbation is greatest aloft. The right-hand panels show a shallow wave, where there is minimal effect on [u,v] at 32 m, but the perturbation in w remains.

3. Results

3.1. Climatology of Events detected by Microbarograph: Extrinsic Velocity

The extrinsic wave direction of the 73 events as detected by microbarograph appear to be bimodal, with an apparent preference for west-bound waves in March, April and May, switching to east bound waves in July through to November (data not shown). The overall wave directions and speeds are given as histograms in figure 6. Most notable in these panels are that the waves rarely come from south or south-east. The velocity histogram shows there is an apparent zone of unobserved waves with low and zero wave speed (relative to the surface). Wave speed distribution is similar in form to the Weibull distribution but with an offset in the x-axis. The red curve overlaid is an optimised Weibull function, with an optimised offset of 1.09 ms^{-1}.

3.2. Climatology of Sodar Signatures

Environmental conditions were suitable for 40 of the events to be visible on corresponding sodar echogrammes. This subset was classified into four general categories, examples of which are shown in the left hand images of figure 7. A description and count of each category is as follows:

- *Bore*: 9 events: a rapid change in the boundary-layer depth as indicated by an abrupt change in the strong echo near the surface
- *Bore-Train*: 8 events: similar to B but with clear wave signature in the deeper side of the event
- *Train*: 15 events: a succession of a few peaks without any apparent bore.
- *Solitary event*: 8 events: a single peak with no associated train

The sodar images categorised as Train events should not be confused with "cats eyes", which are frequently seen in echogrammes of the SBL; cats-eye signature can occur at any height where the sodar return has suitable vertical structure, but are rarely at seen at the surface. They have been identified as Kelvin-Helmholtz billows, generated by internal wind shear aloft. None of the events detected by the pressure signature showed associated cats-eye signature.

4. Discussion

A number of aspects of the waves described in this paper require further discussion, such as how they are generated, how they propagate and do they interact with the turbulence (and hence fluxes) in the SBL. A more complete discussion is to be found in the associated paper in preparation; for this paper, I will discuss possible generation mechanisms, as the data already indicate that these events are universal to SBL flow and are not specific to the Halley site.

The initial formation of these events may be gradual, as per surface waves generated by wind, in which case cause and maintenance are similar mechanisms. Alternatively the wave may be triggered by a catastrophic or acute event, as for pond ripples emanating from a dropped stone; initial cause and subsequent propagation are then separate.

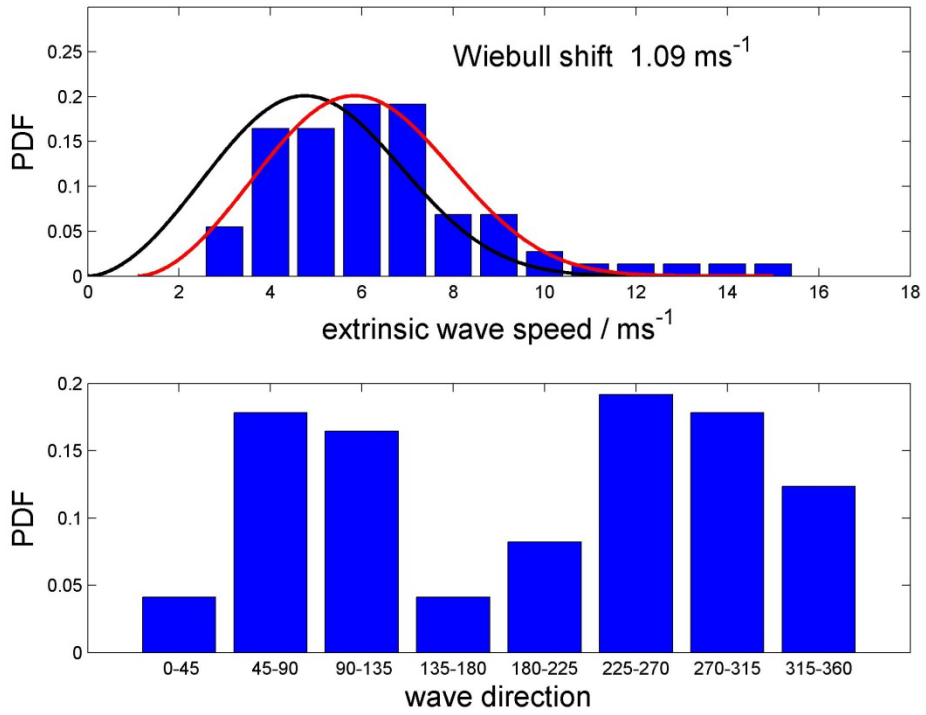

Figure 6. Probability distribution functions (PDFs) for extrinsic (relative to the surface) speed and direction of the waves. The speed PDF fits an offset Weibull distribution (red line) implying there is a limit to the lowest wave velocity. The offset is 1 ms^{-1}. The wave directions are bi-modal, with a minimum in the south and south-east directions. This suggests the waves do not originate from the continent.

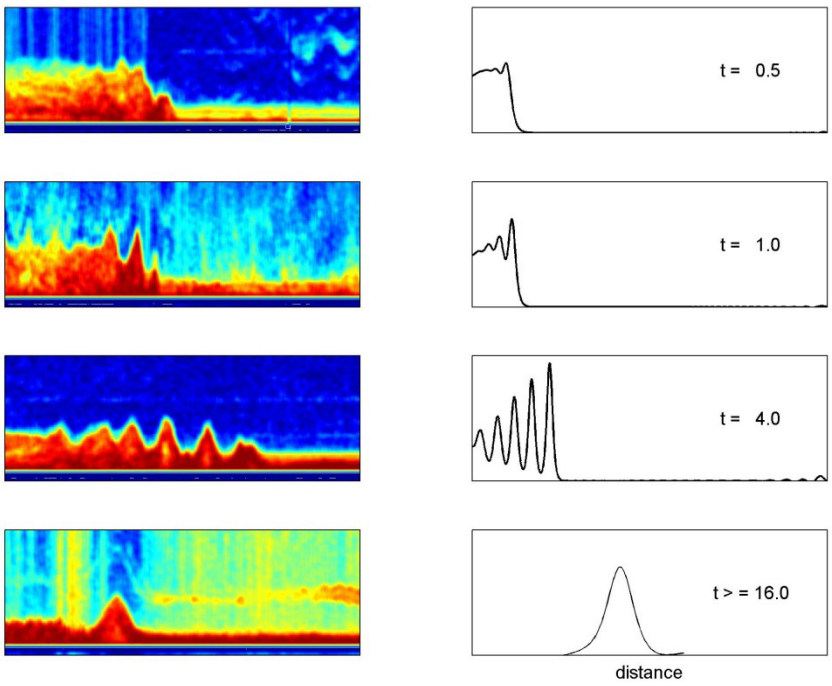

Figure 7. A gallery of four unconnected sodar images, chosen to demonstrate the similarity of their structure to the evolution of the Korteweg – de Vries equation. The equation is initialised as a steep tanh curve which then sheds a train of spreading sech^2 solitons. The similarity to the sodar images is noteworthy but not conclusive, as in situ evolution of the Halley events has not been observed.

The image of some distant cataclysmic event generating atmospheric ripples that then gently traverse the ice shelf is not so far-fetched. Renfrew and Anderson (2002) present AWS observations and modeling of katabatic flows in Coats Land to the south and east of Halley (see figure 2). These flows sudden cease at the grounding line, where the continental ice begins to float, becoming the Brunt Ice Shelf. This sudden (< 1 km) flow cessation is associated with an atmospheric hydraulic jump along the grounding line, which in turn is a source of internal wave activity shedding momentum. The energy involved can indeed be large as the $20ms^{-1}$ katabatic flow some 30 m deep comes to a near standstill, implying a dissipation some 150 kW per metre of coast line.

The climatology of the wave directions presented in figure 6, however, refutes the hydraulic jump as a source of these events, at least for this site. Many events are observed originating from ocean to the north and north-west, or travelling along the ice-shelf parallel to the mean coast. The data appear unaffected by the position of the ice shelf grounding line, and there is no other significant topography in the region.

If local topography is not a factor in the development of the wave signature, the data imply that these waves are inherent and ubiquitous, i.e. they are a universal feature of stratified flow over the ice shelf, and not a peculiarity of the Halley environment. The mechanism for generation (if not necessarily subsequent propagation) must therefore involve interaction within the mean flow, or between the mean flow and the surface.

The events appear to be quite unlike other well documented flow-surface interaction such as surface Kelvin-Helmholtz waves or roll waves. For roll waves, shear is generated by and at the surface drag, and the sense of the resulting vorticity in the wave is the same as for a wheel rolling along a surface. For the events discussed here, the observed vorticity (not shown) is of the opposite sign, that is, the air-mass rotates with minimal shear at the upper interface but with significant shear close to the surface. In this respect, the vorticity is the in the same sense as that observed in fine scale measurements of avalanches (Kern et al. 2010). These in situ measurements of snow-avalanche flow show a "reverse elliptical eddy" within the nose of the avalanche, and also show similar velocity time-series and profiles to those observed in the Halley solitary events.

The similarity between the Halley events and the extreme drainage effects of avalanches is supported by the gallery of 40 sodar echogrammes, from which a family of signatures has been deliberately cherry-picked. The left hand panels of figure 7 show four of these signatures, arranged to indicate a possible aging or evolution of the events. I stress that in reality the signatures are unrelated, and I have chosen them to indicate a hypothesis.

The right hand panels show the actual evolution of the Korteweg-de Vries (KdV) equation initiated with a steep tanh step. The KdV equation (Korteweg and de Vries 1895) was developed to explain the famous 1834 “Wave of Translation” of John Scott Russell, being the first description of a solitary wave. The solitary solutions of the KdV equations show notable similarity in shape to the Halley events that are not distinctly train-like bore-like, suggesting that the dynamics of the ice shelf SBL is similar to a canal. The evolution of the KdV initiated with a tanh step is therefore interesting, and the similarity of certain stages to the observed sodar noteworthy, but in no way conclusive. Furthermore, the KdV model does not offer any suggestion as to the original cause of the supposed drainage flow.

5. Summary and Conclusions

The vorticity of the Halley events appears to minimise shear with the overlying atmosphere, not the surface. As such they appear to be remnants of atmospheric drainage bores or micro-fronts, structurally similar to the extreme density currents of avalanches. The gallery of sodar images support the idea that these events are observations of different ages in the evolution of these fronts. This still begs the question of what initially triggers the drainage-like bores, especially when the wave direction data indicate that they are not originating from the katabatic flows of the continent.

References

Anderson, P.S. (2003) Fine-scale structure observed in a stable atmospheric boundary layer by Sodar and kite-borne tethersonde. *Bound.-Layer Meteor*., **107**(2):323-351.

Anderson, P.S., S.D. Mobbs, J.C. King, I. McConnell and J.M. Rees (1992) A Microbarograph for Internal Gravity-Wave Studies in Antarctica. *Antarctic Science,* **4**(2):241-248.

Christie, D.R. (1992) The morning glory of the Gulf of Carpentaria : a paradigm for non-linear waves in the lower atmosphere. *Australian Meteor. Mag.*, **41**:21-60.

Kern, M.A., P.A. Bartelt and B. Sovilla (2010) Velocity profile inversion in dense avalanche flow. *Ann. Glaciol*,. **51**(54):27-31.

King, J.C. and P.S. Anderson (1988) Installation and Performance of the Stable Instrumentation at Halley. *British Antarctic Survey Bulletin*(79):65-77.

King, J.C., S.D. Mobbs, M.S. Darby and J.M. Rees (1987) Observations of an Internal Gravity-Wave in the Lower Troposphere at Halley, Antarctica. *Bound.-Layer Meteor*., **39**(1-2):1-13.

King, J.C., S.D. Mobbs, J.M. Rees, P.S. Anderson and A.D. Culf (1989) The stable Antarctic boundary layer experiment at Halley Base. *Weather*. **44**: 398-405.

Korteweg, D.J. and F. de Vries (1895) On the Change of Form of Long Waves Advancing in a Rectangular Canal, and on a New Type of Long Stationary Waves. *Philosophical Magazine*. **39**:422-443.

Rees, J.M., P.S. Anderson and J.C. King (1998) Observations of solitary waves in the stable atmospheric boundary layer. *Bound.-Layer Meteor*., **86**(1):47-61.

Rees, J.M. and J.W. Rottman (1994) Analysis of Solitary Disturbances over an Antarctic Ice Shelf. *Bound.-Layer Meteor*., **69**(3):285-310.

Renfrew, I.A. and P.S. Anderson (2002) Observations and numerical modelling of an ordinary katabatic wind regime in Coats Land, Antarctica, *15th Symposium on Boundary Layers and Turbulence*. Amer Meteorological Society, Boston.

Scorer, R.S. (1949) Theory of waves in the lee of mountains. *Quart. J. R. Meteorol. Soc*., **75**:41-56.